

Static and dynamical properties of a magnetic impurity in a strongly correlated electronic system

K. A. Hallberg

Max-Planck-Institut für Physik komplexer Systeme, Bayreuther Str. 40, Haus 16, 01187 Dresden, Germany.

C. A. Balseiro

Centro Atómico Bariloche and Instituto Balseiro, 8400 S. C. de Bariloche, Argentina.

(December 1, 2018)

Abstract

Using numerical techniques we study the zero temperature properties of a substitutional magnetic impurity in a one-dimensional correlated system described by the Hubbard model with repulsive interaction U . We find that, while the static spin correlation maintains a $2k_F$ periodicity, the charge correlations show Friedel oscillations with a $4k_F$ periodicity for large values of U . The static on-site susceptibility decreases as the interactions in the chain are turned on and we interpret this as an increase of the Kondo temperature. For large values of U the short range antiferromagnetic correlations dominate over the collective Kondo singlet formation.

Typeset using REVTeX

Recently much effort has been devoted to the understanding of the effect of impurities in strongly correlated systems [1–3]. However, while the problem of impurities in non-interacting systems like the Kondo [4–6], Anderson [7,8] and Wolff [9] models is well understood, very little is known about the effect that the band correlations may have on the thermodynamic and ground state properties of impurity systems. Some experiments on high-Tc materials [10–12] show the effect of impurities interacting with a strongly correlated $Cu - O$ plane. For instance, heavy fermion behaviour has been observed in $Nd_{1.8}Ce_{0.2}CuO_2$ below $T = 0.3K$ [10]. This behaviour has been modeled by considering a lattice of 4f Nd ions interacting with a system of strongly correlated conduction electrons. The strong anti-ferromagnetic correlations in the $Cu - O$ plane is taken into account by breaking the spin symmetry [3]. Recent theoretical descriptions of the Kondo effect in a Luttinger liquid have been made [13,14] finding an algebraic scaling of the Kondo temperature (T_K) with the Kondo exchange coupling instead of the exponential relation for the conventional Kondo problem in Fermi liquids.

In this paper we perform a finite-size calculation of a single impurity embedded in a correlated electron system. We study the case of a substitutional impurity in a Hubbard ring. We consider a magnetic impurity and present results for the ground state properties such as charge and spin correlation functions as well as dynamical properties: local density of states at the impurity site and frequency dependent spin susceptibility.

The model Hamiltonian reads:

$$H = - \sum_{i,\sigma} t_i (c_{i+1,\sigma}^\dagger c_{i,\sigma} + hc) + U \sum_{i \neq l} n_{i\uparrow} n_{i\downarrow} + U_l n_{l\uparrow} n_{l\downarrow} + \epsilon_l (n_{l\uparrow} + n_{l\downarrow}) \quad (1)$$

Here U_l is the repulsion on the impurity site l , ϵ_l its diagonal energy, $t_{l-1} = t_l = t'$ and $t_i = t$ for all the other sites. Nevertheless we will consider $t' = t = 1$ because we find that the results are qualitatively the same even if $t' \ll t$. As we are interested in a magnetic impurity we take $\epsilon_l \ll -t$ and $\epsilon_l + U_l \gg t$.

We use the Lanczös technique to obtain the ground state of Hamiltonian (1) on an N -site chain with N_e electrons. In order to get a non-degenerate ground state we consider periodic

(antiperiodic) boundary conditions for $N_e/2$ odd (even) (closed shell condition).

In the one-dimensional Hubbard model (in our case it corresponds to $U_l = \epsilon_l = 0$ and $t' = t$) the asymptotic charge and spin correlation functions are given by [15]:

$$\langle n(x)n(0) \rangle = K_\rho/(\pi x)^2 + A_1 \cos(2k_F x)x^{-1-K_\rho} \ln^{-3/2}(x) + A_2 \cos(4k_F x)x^{-4K_\rho} \quad (2)$$

$$\langle \mathbf{S}(x) \cdot \mathbf{S}(0) \rangle = 1/(\pi x)^2 + B_1 \cos(2k_F x)x^{-1-K_\rho} \ln^{1/2}(x) \quad (3)$$

with interaction-dependent parameters A_1 , A_2 , B_1 and K_ρ . For large U it is expected that the $4k_F$ term of the charge correlation function is dominant [16]. This is confirmed by numerical results done in finite systems [17]. As we show below, this behaviour in the correlation functions dominates the charge and spin screening of an impurity embedded in a one-dimensional system.

In Fig. 1 we show results for the static spin ($\langle S_i^z S_j^z \rangle$) and charge ($\langle n_i n_j \rangle$) correlation functions for the quarter filled case for different values of U . We see that the interactions in the chain enhance the antiferromagnetic correlations and the periodicity remains $2k_F$ for the spin correlation. On the other hand, for the charge correlations we find that, as U increases, the amplitude of the oscillations decreases and the main periodicity changes from $2k_F$ to $4k_F$ at $U \simeq 4t$. The behaviour of the system at large U can be understood from the $U = \infty$ limit where the charge dynamics can be described by non-interacting spinless fermions with k_F replaced by $2k_F$. Consequently one expects a contribution proportional to $\cos(4k_F)$ in the density-density correlation functions in this limit. Note that $\langle n_l^2 \rangle \simeq 1$ and $\langle (S_l^z)^2 \rangle \simeq 1/4$ for all U as corresponds to a magnetic impurity with $\epsilon_l \ll -t$ and $\epsilon_l + U_l \gg t$.

We also calculate numerically [18] the density of states at the impurity site $\rho_l(\omega)$. In Fig. 2 we present results for the doped case where the delta peaks have been broadened by a Lorentzian only for visualizing purposes. Important peaks exist close to ϵ_l and $\epsilon_l + U_l$ (the latter ones are out of the range of the figure). The lower and upper Hubbard bands can clearly be recognized for $U = 6t$ (Fig. 2c). A large density of states near the Fermi energy can be seen for all U values. This enhancement is due to the scattering potential introduced by the impurity. Due to the finiteness of the system, we can see two enhanced peaks, one

beneath and one above the Fermi surface but these should become one resonant peak in the infinite system. In the Anderson model (in the spin fluctuating limit) this corresponds to the Kondo resonant peak and its width is proportional to $k_B T_K$. Because we have a finite system it is impossible to extract from these figures the width of the resonant peak. However, we observe that as U increases, the most prominent peaks separate somewhat; this could suggest that the resonant peak gets wider in the thermodynamic limit, implying an increase of the Kondo temperature. For the half filled case the resonant peak at $U = 0$ disappears at finite U due to the formation of the Mott-Hubbard gap. The results presented above are consistent with the dependence of the static spin susceptibility with the interactions of the band presented below.

The local frequency and temperature-dependent spin susceptibility is given by the following expression:

$$\chi'_l(\omega) = \frac{1}{\pi} \int_{-\infty}^{\infty} \tanh\left(\frac{\omega'}{2k_B T}\right) \frac{\text{Im}\langle\langle S_l^+, S_l^- \rangle\rangle_{\omega'+i\delta}^R}{\omega - \omega' + i\delta} d\omega' \quad (4)$$

where $\langle\langle \ \rangle\rangle^R$ is the retarded Green function and χ'_l is in units of $(g\mu_B/2)^2$.

The static and zero temperature limit is:

$$\chi'_l(\omega = 0) = -2\text{Re} \langle\psi_0|S_l^+ \frac{1}{\omega + E_0 - H + i\delta} S_l^- |\psi_0\rangle \Big|_{\omega=0} = 2 \sum_{\nu} \frac{|\langle\nu|S_l^- |\psi_0\rangle|^2}{E_{\nu} - E_0} \quad (5)$$

where $|\psi_0\rangle$ is the ground state of Hamiltonian (1) with energy E_0 and $|\nu\rangle$ and E_{ν} are the excited states and their energies, respectively. This static susceptibility describes essentially the inverse of the difference in energy between the first excited and the ground state (ΔE).

This can be seen by looking at the imaginary part of the response function:

$$\chi''_l(\omega) = -\frac{1}{\pi} \text{Im} \langle\psi_0|S_l^+ \frac{1}{\omega + E_0 - H + i\delta} S_l^- |\psi_0\rangle \quad (6)$$

This is shown in Fig. 3 where we can see that the first excited state has much more weight than the other states of higher energy and is clearly distinguished from them. In the half filled case, instead, the spin excitation spectrum is more complicated but still a clear first excitation peak can be distinguished for small U . We have also checked the spin of the ground state and first excited state, finding they are a singlet and triplet respectively.

For $U = 0$, *i.e.* no correlations in the band, Hamiltonian (1) corresponds to the Wolff model in 1D [9]. In this case it is known that the properties of the system are very similar to those of the Anderson model in the spin fluctuating limit [19]. In particular, as calculated in [20] and checked numerically by us, χ'_l increases with the impurity interaction U_l .

In Fig. 4 we plot the susceptibility as a function of U for several fillings. The case $N_e = 2$ (not shown) is special because one electron is localized at the impurity site so there are no many-body effects on the band. Provided $\epsilon_l \ll -t$ and $\epsilon_l + U_l \gg t$ (as is our case), a simple second-order perturbation calculation shows that ΔE always decreases with U . When more electrons are added to the system and the correlations start playing an important role, we find that χ'_l has a non-monotonic behaviour as a function of U . For small U the susceptibility decreases, it reaches a minimum and then starts to increase. This behaviour can also be seen from (6) where the first peak goes towards higher energies for small U but then tends to zero (very high χ'_l) for large U (see Fig. 3). The susceptibility for the half filled case, instead, always increases with U . The inset of Fig. 4 shows the susceptibility as a function of U for a quarter filled band for $N = 8$ and $N = 12$. Here we see that the lowering of χ'_l for low U is more pronounced for larger systems suggesting that it will be an important feature in the thermodynamic limit.

In conclusion, we have calculated numerically some properties of dilute magnetic impurities embedded in a one-dimensional correlated electronic system. Although we have performed our calculations in a finite system where the low energy characteristics may be missed, this method gives an insight on the properties of the system at zero temperature.

The static correlation functions reflect the non-Fermi liquid behaviour of correlated electrons in one dimension: While the periodicity of the spin-spin correlation remains $2k_F$, the Friedel oscillations in the density-density correlation have a $4k_F$ periodicity at large U . This could probably be measured experimentally with X-ray scattering in doped quasi-one-dimensional systems with dilute impurities.

We also find a large local density of states near the Fermi energy due to the impurity scattering potential. The separation of the most important peaks may indicate that the

width of the resonant peak in the thermodynamic limit increases.

The susceptibility, which measures essentially the inverse of the energy difference between singlet ground state and first excited triplet state (interpreted here as proportional to T_K), shows a non-monotonic behaviour for the doped case. For $U = 0$ a bound singlet state is formed around the impurity [19]. In this non-interacting limit only a small fraction of electrons (those within $k_B T_K$ of the Fermi surface) are involved in the extended singlet state. When the interactions in the band are turned on, the effective mass of the carriers increases, enlarging the density of states near the Fermi energy. As more electrons are involved in the screening of the impurity, the spin compensating cloud becomes more localized and as a consequence, T_K is larger *i.e.* χ'_l decreases. For large U this picture holds no longer because the strong antiferromagnetic correlations inhibit the formation of a collective singlet state around the impurity and the susceptibility increases monotonously. In the half filled case a gap opens for finite U and there is no formation of a collective singlet state around the impurity site and the susceptibility also increases. In this case one expects the susceptibility to diverge at large U (when $U_l \rightarrow \infty$) because conformal field theory studies [21] show that the fixed point of a substitutional spin with antiferromagnetic coupling in a Heisenberg chain is a ‘healed’ Heisenberg chain (with $J = 2t^2/U$).

For the highly doped case, our system is in the Luttinger liquid regime and our results for T_K at small U are qualitatively similar to those of Ref. [14] (small and positive g_2 in their case and small Kondo interaction parameter J). We find that in the Hubbard model the antiferromagnetic correlations play an important role and compete with the collective Kondo singlet formation, dominating at large values of U .

It is interesting to study whether in higher dimensions the features encountered here, *i.e.* the non-monotonous behaviour of the Kondo temperature as a consequence of a competing interaction between Kondo singlet formation and antiferromagnetic interactions, persist. Of course, other methods than exact diagonalization techniques are required. The doubling of the periodicity of the Friedel oscillations in the density-density correlation function is, however, a characteristic of Luttinger liquids.

We would like to thank P. Horsch, H. Eskes, A. Ruckenstein and E. Müller-Hartmann for profitable discussions and especially P. Fulde for valuable discussions and hospitality.

REFERENCES

- [1] M. Ogata and P. W. Anderson, Phys. Rev. Lett. **70**, 3087 (1993).
- [2] D. Poilblanc, W. Hanke and D. J. Scalapino, preprint.
- [3] P. Fulde, V. Zevin and G. Zwicknagl, Zeit. Phys. B **92**, 133 (1993).
- [4] J. Kondo, Prog. Theor. Phys. **28**, 846 (1962).
- [5] N. Andrei, K. Furuya and J. H. Lowenstein, Rev. Mod. Phys. **55**, 331 (1983).
- [6] K. Wilson, Rev. Mod. Phys. **47**, 773 (1975).
- [7] P. W. Anderson, Phys. Rev. **124**, 41 (1961).
- [8] P. B. Wiegmann and A. M. Tsvelick, J. Phys. C, **16**, 2281 (1983).
- [9] P. A. Wolff, Phys. Rev. **124**, 1030 (1961).
- [10] T. Brugger, T. Schreiner, G. Roth, P. Adelman and C. Czjzek, Phys. Rev. Lett. **71**, 2481 (1993).
- [11] W. N. Hardy, D. A. Bonn, D. C. Morgan, R. Liang and K. Zhang, Phys. Rev. Lett. **70**, 399 (1993).
- [12] K. Ishida, Y. Kitaoka, T. Yoshitomi, N. Ogatta, T. Kamino and K. Asayama, Physica C **179**, 29 (1991).
- [13] D. Lee and J. Toner, Phys. Rev. Lett. **69**, 3378 (1992).
- [14] A. Furusaki and N. Nagaosa, Phys. Rev. Lett. **72**, 892 (1994).
- [15] see for example H. J. Schulz, Phys. Rev. Lett. **64**, 2831 (1990); J. Sólyom, Adv. Phys. **28**, 209 (1979).
- [16] Y. Ren and P. W. Anderson, Phys. Rev. B, **48**, 16662 (1993).
- [17] S. Sorella, A. Parola, M. Parrinello and E. Tosatti, Europhys. Lett. **12**, 721 (1990).

- [18] E. Gagliano and C. A. Balseiro, Phys. Rev. Lett. **59**, 2999 (1987).
- [19] P. Schlottmann, Phys. Rev. B, **17**, 2497 (1978).
- [20] V. Zlatić and B. Horvatić, Phys. Rev. B **40**, 3368 (1989).
- [21] S. Eggert and I. Affleck, Phys. Rev. B **46**, 10866 (1992).

FIGURES

FIG. 1. Static spin-spin (a) and density-density (b) correlation functions vs. the distance to the impurity site for $N = 12$, $Ne = 6$ ($k_F = \pi/4$), $U_l = 100t$, $\epsilon_l = -10t$ and $U = 0$ (circles), $U = t$ (squares), $U = 2t$ (diamonds), $U = 4t$ (triangles) and $U = 10t$ (plus).

FIG. 2. Density of states at the impurity site l for $N = 10$, $Ne = 6$, $U_l = 100t$ and $\epsilon_l = -10t$ for $U = 0$ (a), $2t$ (b) and $6t$ (c). Full (dotted) lines: occupied (empty) states.

FIG. 3. $\chi_l''(\omega)$ for the same set of parameters as in Fig. 1 but for $U = 0$ (full line), $U = 4t$ (dotted line) and $U = 30t$ (dashed line)

FIG. 4. Local static susceptibility χ_l' as a function of U for $U_l = 100t$, $\epsilon_l = -10t$, $N = 10$ and different fillings: $Ne = 4$ (full line), 6 (dashed line) and 10 (dashed-dotted). The inset shows χ_l' as a function of U for a quarter filled band for $N = 8$ (lower curve) and $N = 12$ (upper curve), for $U_l = 20t$ and $\epsilon_l = -10t$.

FIG. 1a

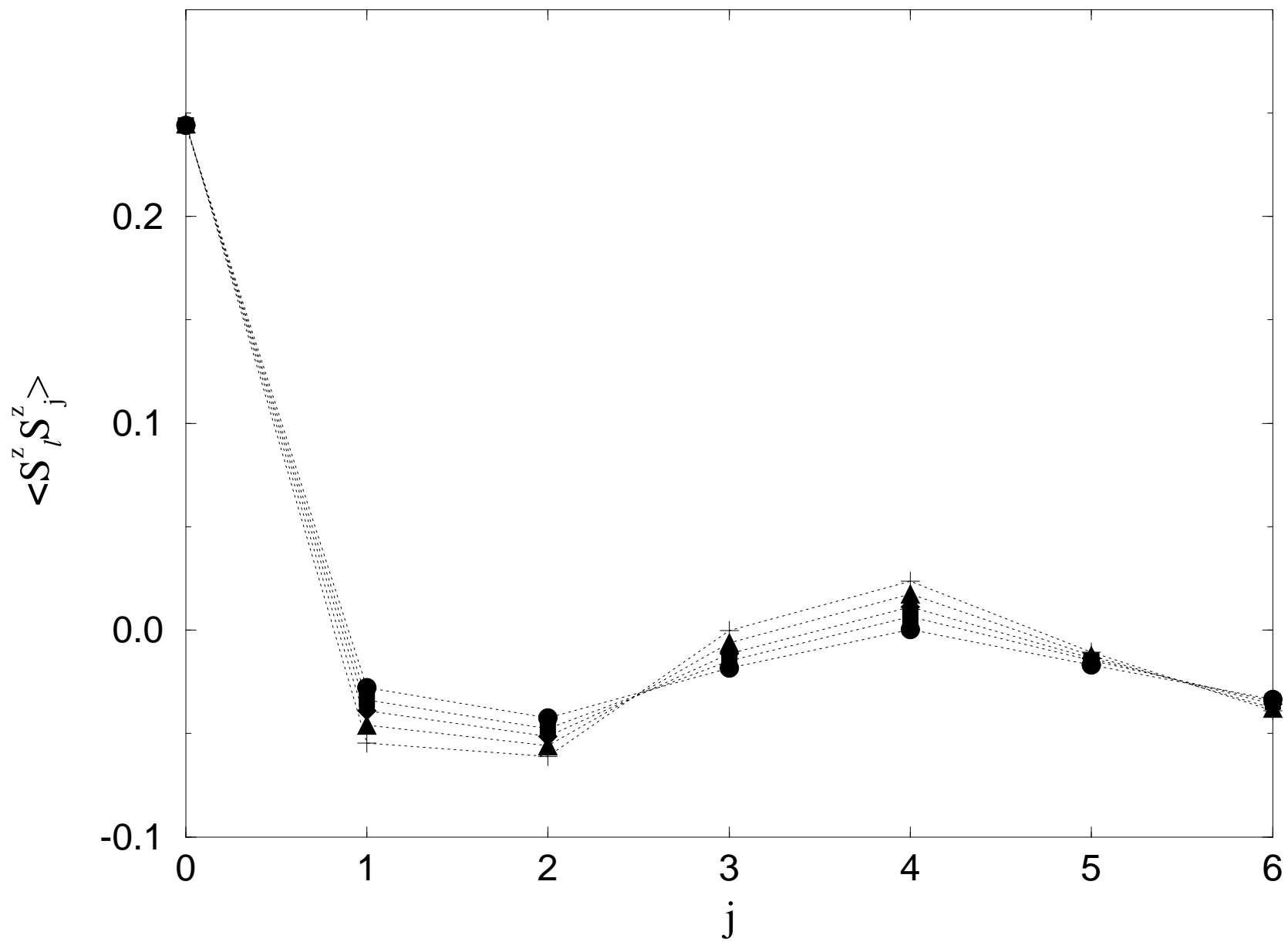


FIG. 1b

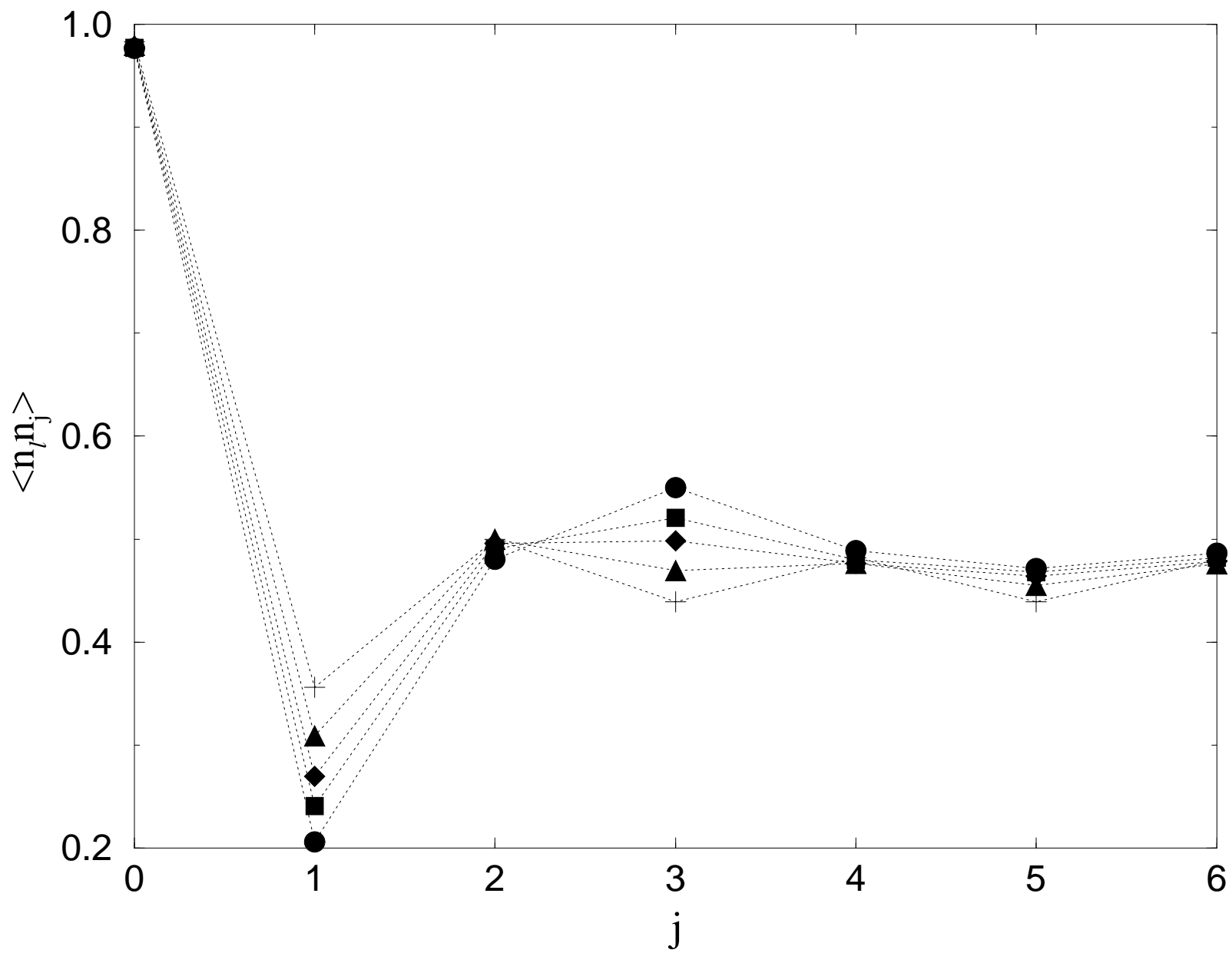


FIG. 2a

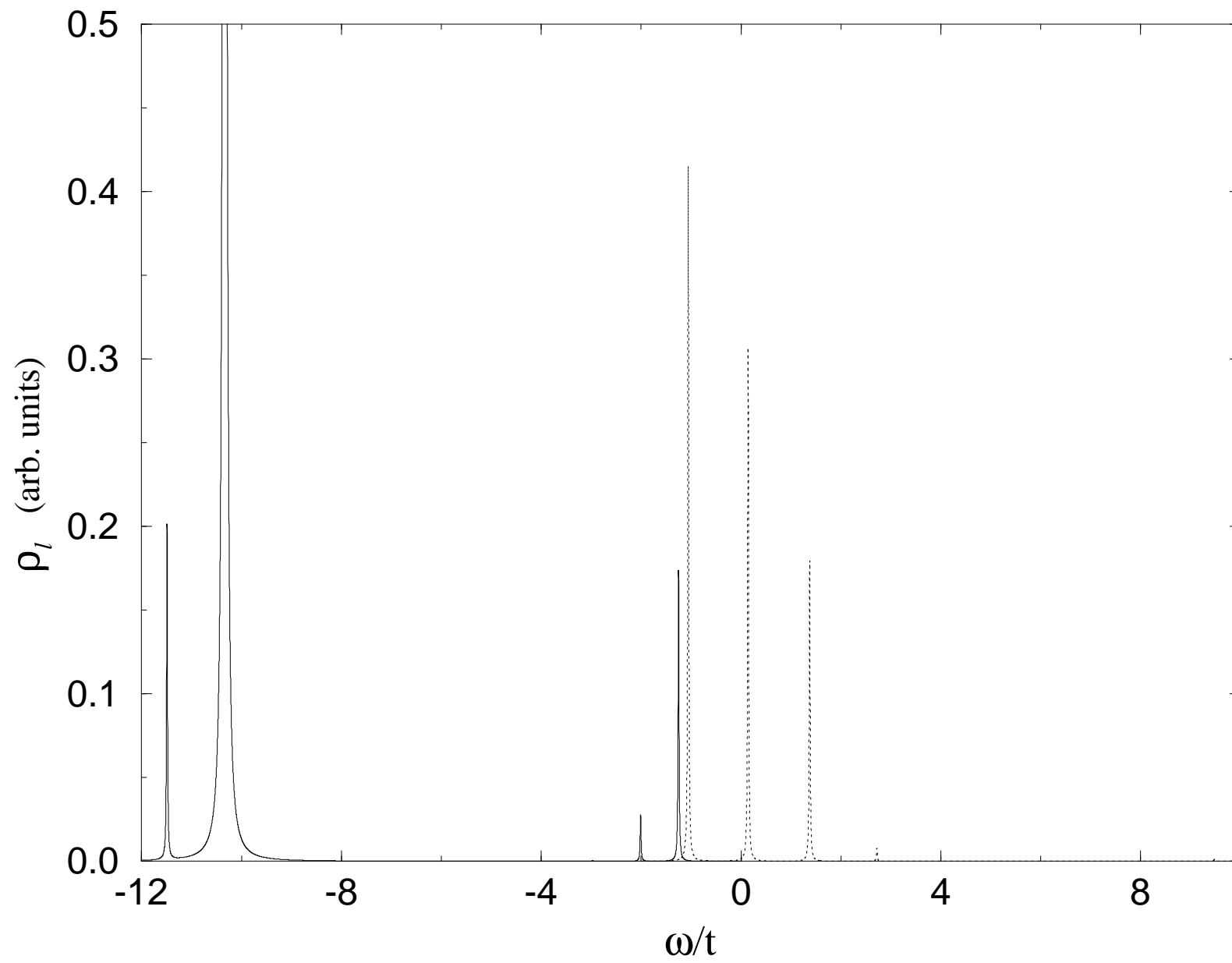


FIG. 2b

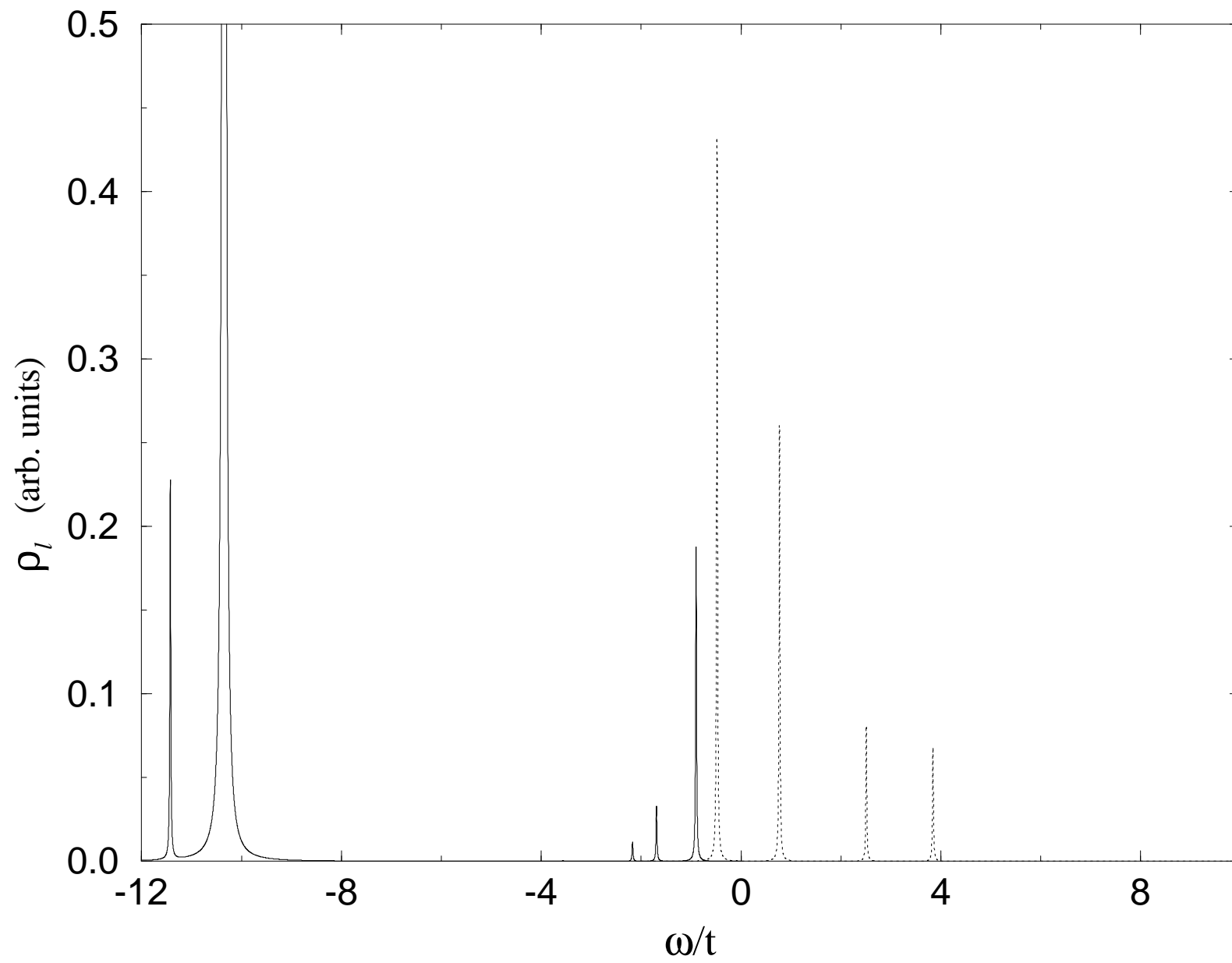


FIG. 2c

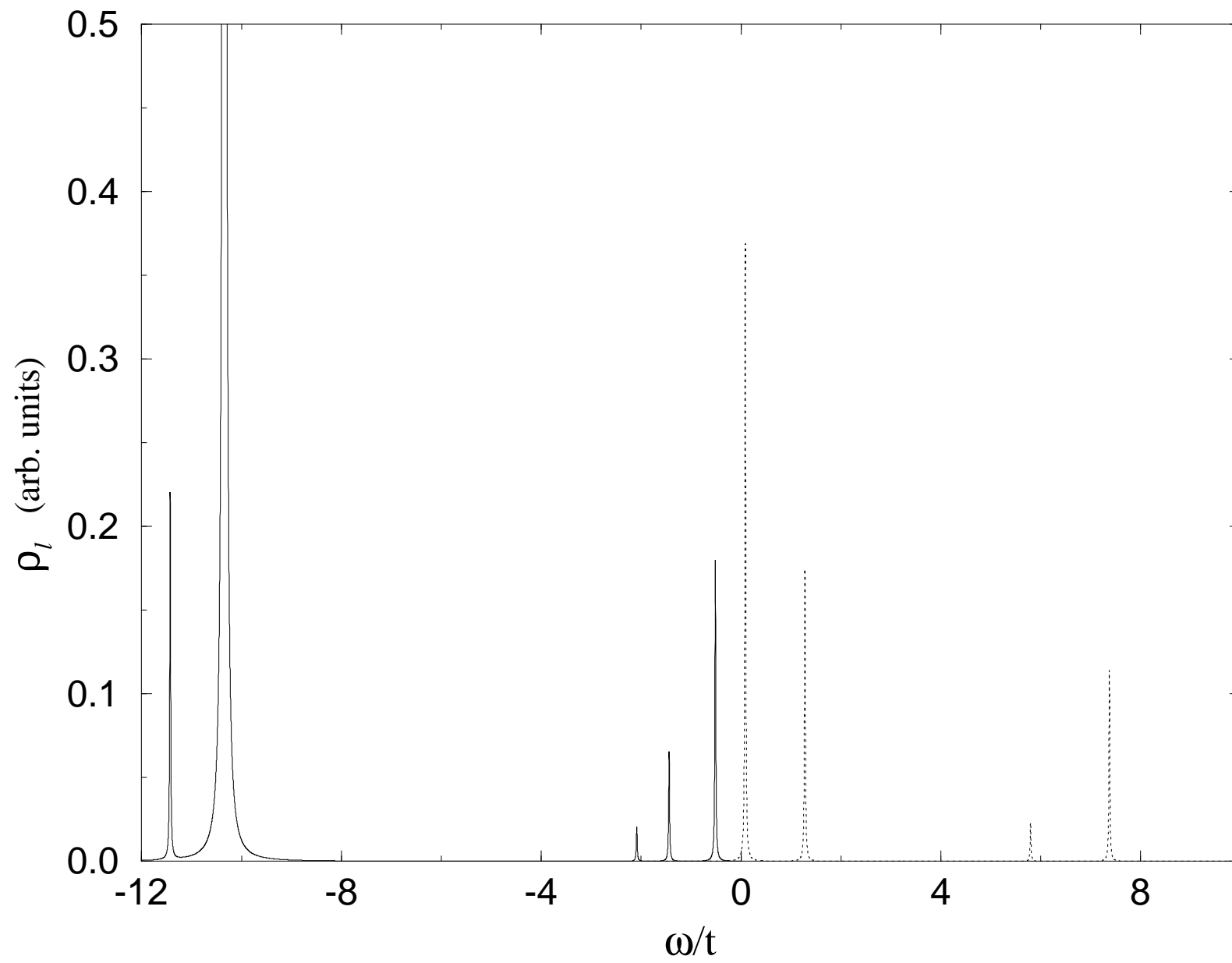


FIG. 3

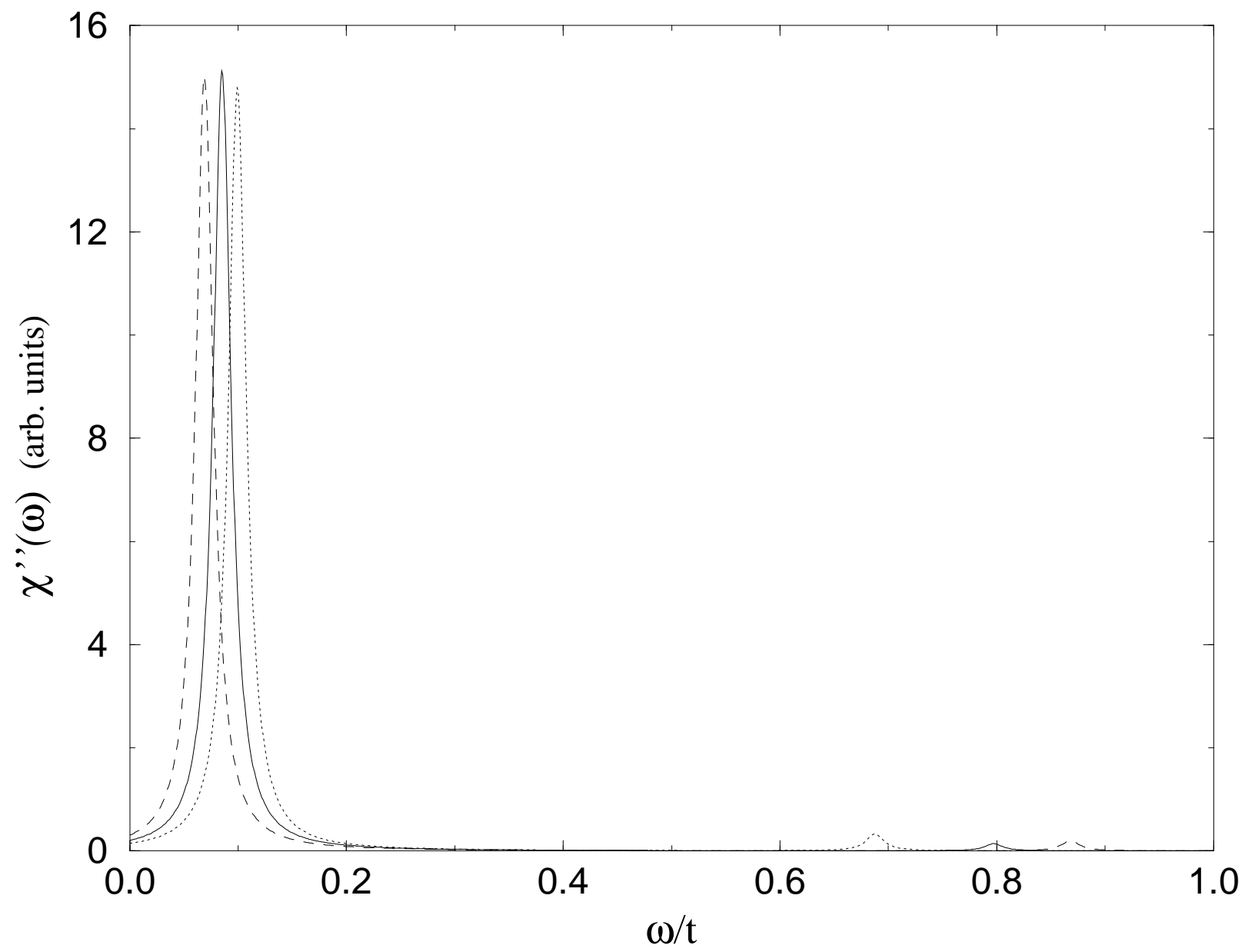


FIG. 4

